

# Trace Metal Speciation by Capillary Electrophoresis Hyphenated to Inductively Coupled Plasma Mass Spectrometry: Sulfate and Chloride Complexes of Np(V) and Pu(V)

Sylvain Topin,<sup>\*,†</sup> Jean Aupiais,<sup>\*,†</sup> Nicolas Baglan,<sup>†</sup> Thomas Vercouter,<sup>‡</sup> Pierre Vitorge,<sup>‡</sup> and Philippe Moisy<sup>§</sup>

CEA, DAM, DIF F-91297 Arpajon, France, CEA, DEN, Saclay, F-91191 Gif-sur-Yvette, France, and CEA, DEN, Valrho BP 17171, 30207 Bagnols sur Ceze, France

In the framework of nuclear waste disposal, it is very important to well understand the behavior of actinides in the presence of the common environmental inorganic ligands such as sulfate and chloride. In this work, the  $\text{AnO}_2\text{SO}_4^-$  and  $\text{AnO}_2\text{Cl} 1-1$  complexes have been evidenced by capillary electrophoresis–inductively coupled plasma mass spectrometry (CE–ICPMS) in perchlorate/chloride and in perchlorate/sulfate media for  $\text{An} = \text{Np}$  and  $\text{Pu}$ . Their binding constants have been measured:  $\log \beta_{\text{PuO}_2\text{SO}_4^-}^0 = 1.30 \pm 0.11$ ,  $\log \beta_{\text{PuO}_2\text{Cl}}^{\text{LM,NaCl}} = -(0.40 \pm 0.07)$ ,  $\log \beta_{\text{NpO}_2\text{SO}_4^-}^0 = 1.34 \pm 0.12$ , and  $\log \beta_{\text{NpO}_2\text{Cl}}^{\text{LM,NaCl}} = -(0.40 \pm 0.07)$ . These results are consistent with published values for Np(V). They confirm the expected analogy between Np(V) and Pu(V) for the weak bonding with chloride ligand,  $\log_{10} \beta_{\text{PuO}_2\text{Cl}} \approx \log_{10} \beta_{\text{NpO}_2\text{Cl}}$ , attributed to mainly electrostatic interactions. Conversely, a slight shift is observed for the bonding with sulfate ligand,  $\log_{10} \beta_{\text{NpO}_2\text{SO}_4^-} > \log_{10} \beta_{\text{PuO}_2\text{SO}_4^-}$ , indicating that some covalency might stabilize the sulfate complexes.

Actinides are usually chemical analogues when in the same oxidation state, i.e., forming cations of the same charge and similar sizes, which form complexes of the same stoichiometry and similar stabilities. This analogy is often used to predict the chemistry of actinides in oxidation states when they are difficult to study. It is typically the case for the actinides at the +5 oxidation state among which protactinium, neptunium, and plutonium can be stabilized in the environment. Indeed, the soluble Pu(V) can be quite stable at trace concentrations in environmental surface waters, and its aqueous chemistry is essentially known by analogy with Np(V), which is the most stable An(V).<sup>1</sup> Conversely, Pa(V) is not a chemical analogue of the other An(V) ions since it has been

recently shown that its aqua ion is not of the same form.<sup>2–4</sup> Therefore, it seems that such analogy rules need experimental verifications. Only few thermodynamical data are published for plutonium and protactinium in the +5 oxidation state (Pu(V) and Pa(V)), while more data are available in the literature for Np(V).<sup>1</sup> Np(V) is stable as the linear  $\text{NpO}_2^+$  neptunyl ion with solvent or ligand molecules in its equatorial plan. The Pu(V) aqua ion has a similar structure and a size close to that of Np(V), and the available complexing constants are similar for Np(V) and Pu(V).<sup>1</sup> Furthermore, Pu(V) is the second more stable An(V) after Np(V); therefore, their behavior versus complexation is compared here.

The complexation can be driven by two components: electrostatic interactions including possible outer sphere interactions and covalent bonding which exists only in inner sphere complexes. The electrostatic interactions between Np(V) and anionic ligands might be slightly weaker than those for Pu(V), since its density of charge is smaller. Conversely, Np covalent binding with anions might be stronger than for Pu since the 5f electrons of Np (electrons which participate in the bond) are less localized. The only binding constants selected by the NEA review<sup>1</sup> for both Np(V) and Pu(V) are for carbonate complexes:  $\log_{10} \beta_{\text{AnO}_2\text{CO}_3^-}^0 = 5.12 \pm 0.06$  and  $4.96 \pm 0.06$  for  $\text{An} = \text{Pu}$  and  $\text{Np}$ , respectively. The Pu complex is slightly more stable, but the difference is only a little more than the uncertainties. We recently measured similar values ( $\log_{10} \beta_{\text{AnO}_2\text{CO}_3^-}^0 = 4.95 \pm 0.10$  and  $4.88 \pm 0.12$  for  $\text{An} = \text{Pu}$  and  $\text{Np}$ , respectively) by capillary electrophoresis–inductively coupled plasma mass spectrometry (CE–ICPMS).<sup>5</sup> Conversely, Moskvina et al. proposed slightly more stable  $\text{HPO}_4^{2-}$  complexes with Np(V) than with Pu(V):  $\log_{10} \beta_{\text{NpO}_2\text{HPO}_4^-} = 2.90 \pm 0.11 > \log_{10} \beta_{\text{PuO}_2\text{HPO}_4^-} = 2.39 \pm 0.04$ .<sup>6</sup> The  $\log_{10} \beta_{\text{NpO}_2\text{HPO}_4^-} - \log_{10} \beta_{\text{PuO}_2\text{HPO}_4^-} = 0.51$  difference cannot be explained by the sizes of the cations: it might evidence some covalent character. However, those complexing constants were

\* To whom correspondence should be addressed. E-mail: sylvain.topin@cea.fr (S.T.); jean.aupiais@cea.fr (J.A.).

<sup>†</sup> CEA, DAM, DIF F-91297 Arpajon.

<sup>‡</sup> CEA, DEN, Saclay, F-91191 Gif-sur-Yvette.

<sup>§</sup> CEA, DEN, Valrho BP 17171, 30207 Bagnols sur Ceze.

(1) Lemire, R. J. *Chemical Thermodynamics of Neptunium and Plutonium*, OECD Nuclear Energy Agency, Data Bank, Ed.; Elsevier: Amsterdam, The Netherlands, 2001; Vol. 4, p 845.

(2) Toraiishi, T.; Tsuneda, T.; Tanaka, S. *J. Phys. Chem. A* **2006**, *110* (49), 13303–13309.

(3) Le Naour, C.; Trubert, D.; Di Giandomenico, M. V.; Fillaux, C.; Den Auwer, C.; Moisy, P.; Hennig, C. *Inorg. Chem.* **2005**, *44* (25), 9542–9546.

(4) Siboulet, B.; Marsden, C. J.; Vitorge, P. *New J. Chem.* **2008**, *32* (12), 2080–2394.

(5) Topin, S.; Aupiais, J.; Moisy, P. *Electrophoresis* **2009**, *30*, 1747–1755.

(6) Moskvina, A. I.; Poznyakov, A. N. *Russ. J. Inorg. Chem.* **1979**, *24*, 1357–1362.

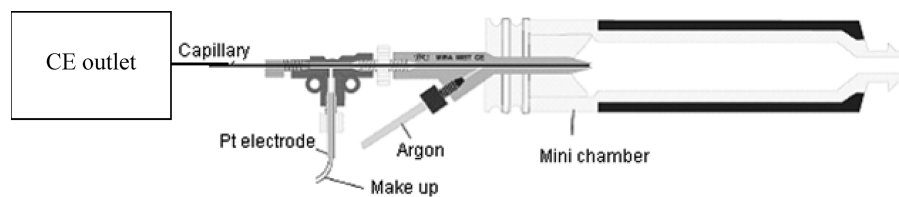
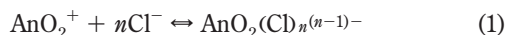


**Figure 1.** Burgener research interface, Mira Mist CE, linking capillary electrophoresis and ICPMS.

criticized and not recommended by the NEA review.<sup>1</sup> For the weakest interactions (chloride, nitrate, ...), the thermodynamical data are scarce. Indeed, no data are available for Pu(V) and only few data are cited for Np(V).<sup>1,7</sup> The small values of the binding constants of Np(V) with the chloride and the nitrate ions proposed in the literature are likely due to small interionic interactions and make it difficult to measure them.

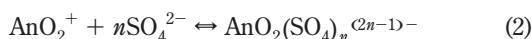
In this study, Np(V) and Pu(V) are investigated in chloride and sulfate aqueous solutions for several reasons. (1) We first want to confirm the Np(V)/Pu(V) analogy is justified by several points. (2) The NEA review did not find reliable published formation constants for the corresponding complexes of Pu(V).<sup>1,7</sup> (3) Pu(V) is stable enough in chloride and sulfate media, and qualitative comparison of Np and Pu is a classical mean to check the +5 oxidation state of Pu. (4) The An(V)–chloride complexes are weak, likely due to electrostatic interactions while the sulfate complexes are more stable, certainly corresponding to inner sphere interactions.<sup>8</sup>

The An(V)–chloride interaction



is extremely weak:  $\log_{10} \beta_{\text{AnO}_2\text{Cl}} = -(0.29 \pm 0.05)$ ,<sup>9</sup>  $-(0.42 \pm 0.04)$ ,<sup>10</sup>  $0.48$ ,<sup>11</sup>  $-(0.05 \pm 0.02)$ , and  $-(0.71 \pm 0.04)$ .<sup>12</sup> Moreover, the structural investigations (X-ray absorption fine structure (XAFS)<sup>13</sup> and spectrophotometry<sup>12,14</sup>) have shown that there is no direct binding of Np(V) with  $\text{Cl}^-$  when  $[\text{Cl}^-] < 5 \text{ mol L}^{-1}$  indicating that no inner sphere interactions occur. The investigation of this interaction has a special interest for the management of the waste in the geological repositories (salt mine of Gorleben and Asse (Germany)).

The An(V)–sulfate interaction



is stronger than for chloride but still low:  $-0.10 < \log_{10} \beta_{\text{NpO}_2\text{SO}_4^-} < 0.76$ .<sup>8,10,11,15</sup> Halperin et al. proposed that this reaction is entropy

driven (positive entropy and enthalpy), which they interpreted as originating in the substitution of a water molecule of the first hydration sphere of An(V) with a sulfate ion (inner sphere complexation).<sup>8</sup>

The +5 oxidation state of plutonium is predicted to play a key role in oxidizing conditions (surface waters). The Pu(V) concentration in natural water depends on the equilibrium with the insoluble form  $\text{Pu}(\text{OH})_4$ . Pu(V) has been measured as the main plutonium oxidation state in several oxic waters.<sup>16–18</sup> Besides, the  $\text{PuO}_2^+$  monocation of Pu(V) is the less reactive form of Pu aquo ions:  $\text{PuO}_2^+ < \text{PuO}_2^{2+} \approx \text{Pu}^{3+} < \text{Pu}^{4+}$ . It results in a high mobility of Pu(V) in the environment.

Partition techniques (liquid–liquid extraction, coprecipitation, ion exchange, ...) are usually well suited to study weak interactions and have been widely used to investigate the Np(V) complexation by inorganic ligands.<sup>6,8–12,15</sup> Nevertheless, the interaction with another phase can destabilize Pu(V). In this work, we used another partition technique: capillary electrophoresis. This technique has been commonly employed to extrapolate binding constants in the biological field.<sup>19</sup> Note that it allows to check the charges of the mobile species *in situ*, hence, their oxidation states. Coupling ICPMS to CE allows measurements at the trace level, close to the environmental level,<sup>20</sup> below the solubility limit. Trace concentrations also hamper the disproportionation of Pu(V).

CE–ICPMS instrumentation has had lots of improvements since 1995 and the first work by Olesik et al.<sup>21</sup> It can be considered now as robust and sensitive, and especially thanks to the commercial interface from Burgener Research, which was developed in order to better adapt CE to ICPMS.<sup>22</sup> This interface uses a parallel path micronebulizer (Mira Mist CE), which prevents the suction effect and operates at low flow rate. The association of this nebulizer with an efficient spray mini-chamber (Figure 1) provides a high-resolution and sensitive tool. Several works have demonstrated the capability of CE–ICPMS to investigate actinide complexation without any change of the speciation during the separation.<sup>5,23,24</sup> In addition, Philippini and co-workers have also demonstrated the capability to perform separation at high ionic

(7) Morss, R. L.; Edelstein, N. M.; Fuger, J. *The Chemistry of the Actinide and Transactinide Elements*, 3rd ed.; Springer: Dordrecht, The Netherlands, 2006; Vol. 2, p 699.  
 (8) Halperin, J.; Oliver, J. H. *Radiochem. Acta* **1983**, *33*, 29–33.  
 (9) Gainar, I.; Skyes, K. W. *J. Chem. Soc.* **1964**, 4452–4459.  
 (10) Rao, P. R. V.; Gudi, N. M.; Bagawde, S. V.; Patil, S. K. *J. Inorg. Nucl. Chem.* **1979**, *41*, 235–239.  
 (11) Patil, S. K.; Ramakrishna, V. V.; Gudi, N. M. *Proc. Nucl. Chem. Radiochem. Symp.*, Varansi, India, November 3–7, 1981, Indian Department of Atomic Energy, 1981; pp 388–390.  
 (12) Neck, V.; Kim, J. I.; Kannellakopoulos, B. *Thermodynamisches Verhalten von Neptunium(V) in konzentrierten NaCl- und NaClO<sub>4</sub>-Lösungen*; Tech. Rep. Kfk 5301, Kernforschungszentrum Karlsruhe: Karlsruhe, Germany, 1994; p 37.  
 (13) Allen, P. G.; Bucher, J. J.; Shuh, D. K.; Edelstein, N. M.; Reich, T. *Inorg. Chem.* **1997**, *36*, 4676–4683.

(14) Giffaut, E. Influence des Ions Chlorure sur la Chimie des Actinides. Effets de la Radiolyse et de la Température. Thesis, Paris 11, Orsay, 1994.  
 (15) Inoue, Y.; Tochiyama, O. *Bull. Chem. Soc. Jpn.* **1985**, *58*, 2228–2233.  
 (16) Orlandini, K. A.; Penrose, W. R.; Nelson, D. M. *Mar. Chem.* **1986**, *18*, 49–57.  
 (17) Bondietti, E. A.; Trabalka, J. R. *Radiochem. Radioanal. Lett.* **1980**, *42* (3), 169–176.  
 (18) Choppin, G. R. *Radiochim. Acta* **2003**, *91*, 645–649.  
 (19) Rundlett, K. L.; Armstrong, D. W. *Electrophoresis* **1997**, *18*, 2194–2202.  
 (20) Baglan, N.; Hemet, P.; Pointurier, F.; Chiappini, R. *J. Radioanal. Nucl. Chem.* **2004**, *261* (3), 607–617.  
 (21) Olesik, J. W.; Kinzer, J. A.; Olesik, S. V. *Anal. Chem.* **1995**, *67*, 1–12.  
 (22) Yanes, E. G.; Miller-Ihli, N. J. *Spectrochim. Acta B* **2004**, *59*, 883–890.  
 (23) Kuczewski, B.; Marquardt, C. M.; Seibert, A.; Geckeis, H.; Kratz, J. V.; Trautmann, N. *Anal. Chem.* **2003**, *75* (24), 6769–6774.  
 (24) Ambard, C.; Delorme, A.; Baglan, N.; Aupiais, J.; Pointurier, F.; Madic, C. *Radiochim. Acta* **2005**, *93* (11), 665–673.

strength, e.g., 1.5 M, allowing one to perform experiments with a large amount of ligands.<sup>25</sup> A methodology, used in CE especially in the biological field, is applied to assess the unknown binding constants.<sup>19</sup>

In this work, the CE–ICPMS instrumentation is applied to determine the unknown thermodynamical data relative to the interaction between Pu(V) and inorganic ligands (sulfate, chloride) and to compare to those provided in the literature for Np(V) to check the analogy Pu(V)/Np(V).

## TREATMENT OF DATA

**Determination of Electrophoretic and Electro-Osmotic Mobilities.** The velocity of an ionic metal M ( $v_M$ ) in capillary electrophoresis is calculated as

$$v_M = \mu_M E$$

where  $\mu_M$  ( $\text{cm}^2 \text{s}^{-1} \text{V}^{-1}$ ) is the electrophoretic mobility and  $E$  is the electric field applied between the capillary inlet and the capillary outlet. The electrophoretic mobility was determined experimentally by using

$$\mu = \frac{Ll}{V} \left( \frac{1}{t_M} - \frac{1}{t_{\text{eof}}} \right) \quad (3)$$

where  $L$  (cm) is the total length of the capillary,  $l$  (cm) the length between the capillary inlet and the detection window,  $t_M$  (s) the migration time of the species M between the injection and the channeltron detection of the ICPMS, and  $t_{\text{eof}}$  (s) the migration time of the *N,N*-dimethylformamide (DMF) (neutral species which is used to determine the electro-osmotic flow (eof)) between the injection and the UV detection at the distance  $l$ .

Both migration times,  $t_M$  and  $t_{\text{eof}}$ , were determined simultaneously from three replicates assuming a Gaussian shape of the peaks. The uncertainty associated with the position of the peak was better than 0.5 s. It results in a relative uncertainty lower than 5%.

The effect of the substitution of  $\text{NaClO}_4$  by  $\text{Na}_2\text{SO}_4$  or  $\text{NaCl}$  on the mobilities<sup>26</sup> has been neglected because the media properties are close for  $\text{NaCl}$  and  $\text{NaClO}_4$ , and the change is not significant between 100%  $\text{NaClO}_4$  and the mixture  $\text{Na}_2\text{SO}_4/\text{NaClO}_4$  (20%/80% for the highest concentration in sulfate ligand).

**Determination of Binding Constants.** Two kind of complexes must be distinguished in CE.<sup>27</sup> (1) The strong complexes are usually not dissociated during the separation, and each species is characterized by a specific peak on the electropherogram. (2) The labile complexes are usually characterized by high kinetics of formation and dissociation. In this case, there is a permanent and fast ligand exchange resulting in a single average peak whose position is characteristic of the equilibrium between the metal ion M and the complexes  $\text{ML}_i$ .

In practice, the labile complexes need to add the ligand into the electrolyte to avoid its dissociation. In the case of the labile complexes, the overall electrophoretic mobility

$$\mu_{\text{ov}} = \sum_j (\alpha_j \mu_j) \quad (4)$$

was determined by the ( $\mu_j$ ) individual electrophoretic mobilities and by the ( $\alpha_j$ ) proportions of the different chemical forms ( $j$ ). Thus, for a system of  $n$  complexes

$$\mu_{\text{ov}} = \frac{\mu_M + \sum_{i=1}^n \beta_{\text{ML}_i} [\text{L}]^i \mu_{\text{ML}_i}}{1 + \sum_{i=1}^n \beta_{\text{ML}_i} [\text{L}]^i} \quad (5)$$

where  $[\text{L}]$  is the ligand concentration and  $\beta_{\text{ML}_i}$  is the binding constant of  $\text{ML}_i$ .

The  $\mu_{\text{ov}}$  data were fitted using eq 5 where  $\mu_M$  was measured in absence of ligand whereas the mobilities  $\mu_{\text{ML}_i}$  of the complexes  $\text{ML}_i$  were roughly assessed according to the model of Anderko et al.,<sup>28</sup>

$$\lambda_{\text{complex}}^0 = \frac{|z_{\text{complex}}|}{\left[ \sum_{i=1}^n \left( \frac{z_i}{\lambda_i^0} \right)^3 \right]^{1/3}} \quad (6)$$

$\lambda_{\text{complex}}^0$  and  $z_{\text{complex}}$  refers to the limiting conductivity and the charge of the complex,  $\lambda_i^0$  and  $z_i$  refers to the limiting conductivities and the charges of the species  $i$ , constitutive of the complex. The relation between the limiting conductivity and the electrophoretic mobility is given by

$$\mu^0 = \frac{\lambda^0}{F} \quad (7)$$

where  $F$  is the Faraday constant. The consistency of each mobility was roughly checked by a comparison with literature data for species of similar charge to size ratio when available. An uncertainty of  $\pm 25\%$  is considered for the calculation of  $\mu_{\text{ML}_i}$ , based on the maximal deviation observed between several kinds of complexes.<sup>28</sup> However,  $\mu_{\text{ML}_i}$  has not been used as a constant but as a free parameter varying within its uncertainties. It allowed one to extrapolate upper and lower values for  $\beta_{\text{ML}_i}$ . The average value is selected, and the half of this interval corresponds to the uncertainty. It must be noted that the uncertainties associated with  $\mu_M$ ,  $\mu_{\text{ov}}$ , and  $[\text{L}]$  are negligible regarding the uncertainties associated with  $\mu_{\text{ML}_i}$ .

In the case of sulfate complexation, the mobilities of  $\text{AnO}_2\text{SO}_4^-$ ,  $\mu_{\text{AnO}_2\text{SO}_4^-}$ , have been estimated between  $I_m = 0.357 \text{ mol kg}^{-1}$  and  $I_m = 1.617 \text{ mol kg}^{-1}$  using eqs 6 and 7 (Table 1). The values are similar for both Np and Pu complexes at each ionic strength. They were confidently used since they are close to the similar  $\text{NpO}_2\text{CO}_3^-$  complex, previously determined:<sup>29</sup>  $\mu_{\text{NpO}_2\text{CO}_3^-} = -(2.12 \pm 0.14) \times 10^{-4} \text{ cm}^2 \text{V}^{-1} \text{ s}^{-1}$ .

In the case of chloride complexation, the mobility of  $\text{AnO}_2\text{Cl}$  is zero (neutral species) and eq 5 is written as  $\mu_{\text{ov}} = (\mu_{\text{AnO}_2^+}) / (1 + \beta_{\text{AnO}_2\text{Cl}} [\text{Cl}^-])$ .

(25) Philipini, V.; Vercouter, T.; Aupiais, J.; Topin, S.; Ambard, C.; Chaussé, A.; Vitorge, P. *Electrophoresis* **2008**, *29* (10), 2041–2050.

(26) Onsager, L.; Fuoss, R. J. *Phys. Chem.* **1932**, *36*, 2689–2778.

(27) Sonke, J. E.; Salters, V. J. M. *Analyst* **2004**, *129* (8), 731–738.

(28) Anderko, A.; Lencka, M. M. *Ind. Eng. Chem. Res.* **1997**, *36*, 1932–1943.

(29) Ambard, C. La Spéciation du Plutonium à l'États de Traces par le Couplage Électrophorèse Capillaire-Spectrométrie de Masse à Source Plasma Couplée par Induction. Thesis, Paris 11, Orsay, 2007.

**Table 1. Experimental Values of the Mobility of  $\text{SO}_4^{2-}$ ,  $\mu_{\text{SO}_4^{2-}}$ , in NaCl Medium<sup>a</sup>**

$I_m$ (mol kg <sup>-1</sup> )	$\mu_{\text{SO}_4^{2-}} \times 10^4$ (cm <sup>2</sup> s <sup>-1</sup> V <sup>-1</sup> )	$\mu_{\text{NpO}_2\text{SO}_4^-} \times 10^4$ (cm <sup>2</sup> s <sup>-1</sup> V <sup>-1</sup> )	$\mu_{\text{PuO}_2\text{SO}_4^-} \times 10^4$ (cm <sup>2</sup> s <sup>-1</sup> V <sup>-1</sup> )
0.357	-(4.73 ± 0.10)	-(1.88 ± 0.45)	-(1.90 ± 0.47)
0.725	-(4.18 ± 0.05)	-(1.74 ± 0.42)	-(1.75 ± 0.44)
1.051	-(3.94 ± 0.03)	-(1.69 ± 0.41)	-(1.70 ± 0.42)
1.617	-(3.94 ± 0.09)	-(1.69 ± 0.41)	-(1.70 ± 0.42)

<sup>a</sup> Estimation of the mobility of  $\text{AnO}_2\text{SO}_4^-$  (An = Np, Pu).<sup>28</sup> The  $\text{NaClO}_4$  medium was not used here, since it precipitates with the reverse-eof reagent, TTAB.

**Extrapolation to Zero Ionic Strength.** The specific interaction theory (SIT), as developed by NEA,<sup>1</sup> was used to extrapolate the constants to zero ionic strength. The SIT formula is

$$\log \beta_{\text{ML}_i} - \Delta z^2 D = \log \beta_{\text{ML}_i}^0 - \Delta(\varepsilon_{ij} m_j) \quad (8)$$

where  $D = 0.509 I_m^{1/2} / (1 + 1.5 I_m^{1/2})$  (at 1 bar and 25 °C) is a Debye–Hückel term,  $I_m$  is the ionic strength in molal units,  $\varepsilon_{ij}$  is the pair interaction coefficient between ions  $i$  and  $j$ ,  $m_j$  is the molality of the species  $j$ , and  $\Delta z^2 = (z_M - n z_L)^2 - z_M^2 - n z_L^2$ , where  $(z_M - n z_L)$ ,  $z_M$ , and  $z_L$  are the charges of  $\text{ML}_m$ ,  $M$ , and  $L$ , respectively.

When considering the background electrolyte,

$$\Delta(\varepsilon_{ij} m_j) = -\varepsilon_{\text{Cl}^-, \text{Na}^+} m_{\text{Na}^+} - \varepsilon_{\text{AnO}_2^+, \text{ClO}_4^-} m_{\text{ClO}_4^-} - \varepsilon_{\text{AnO}_2^+, \text{Cl}^-} m_{\text{Cl}^-} \quad (9)$$

for the equilibrium in eq 1 and

$$\Delta(\varepsilon_{ij} m_j) = \varepsilon_{\text{AnO}_2\text{SO}_4^-, \text{Na}^+} m_{\text{Na}^+} - \varepsilon_{\text{SO}_4^{2-}, \text{Na}^+} m_{\text{Na}^+} - \varepsilon_{\text{AnO}_2^+, \text{ClO}_4^-} m_{\text{ClO}_4^-} - \varepsilon_{\text{AnO}_2^+, \text{SO}_4^{2-}} m_{\text{SO}_4^{2-}} \quad (10)$$

for the equilibrium in eq 2.<sup>30</sup> The influence of the others species ( $\text{H}^+$ ,  $\text{OH}^-$ ,  $\text{HSO}_4^-$ ,  $\text{CO}_3^{2-}$ ) was neglected (pH ≈ 6). For each experiment, the value of  $\Delta(\varepsilon_{ij} m_j)$  was calculated using the  $\varepsilon_{ij}$  values tabulated by NEA and/or estimated when unknown (Table 2). Several empirical methods were used to assess these unknown coefficients.<sup>31,32</sup> The  $\varepsilon_{ij}$  parameters of complexes were estimated thanks to a relation established by Ciavatta.<sup>31</sup> For a dipolar ionic species, the positive pole, generally centered on the metal ion, is surrounded by a semispherical cloud of the anions of the medium. The effect may be considered as approximately 50% of the spherical distribution around the metal ion. Moreover, the same consideration is applied at the negative pole. It results in a rough estimation of  $\varepsilon_{\text{ML}_m\text{XN}}$  as the average of  $\varepsilon_{\text{M}_m\text{X}}$  and  $\varepsilon_{\text{N}_m\text{L}}$

$$\varepsilon_{\text{ML}_m\text{XN}} = \frac{\varepsilon_{\text{M}_m\text{X}} + \varepsilon_{\text{N}_m\text{L}}}{2} \quad (11)$$

(30) Vercouter, T.; Amekraz, B.; Moulin, C.; Giffaut, E.; Vitorge, P. *Inorg. Chem.* **2005**, *44*, 7570–7581.

(31) Ciavatta, L. *Ann. Chim.* **1990**, *80*, 255–263.

(32) Vitorge, P.; Phrommavanh, V.; Siboulet, B.; You, D.; Vercouter, T.; Descotes, M.; Marsden, C. J.; Beaucaire, C.; Gaudet, J.-P. *C. R. Chim.* **2007**, *10*, 978–993.

**Table 2. SIT Interaction Coefficient  $\varepsilon_{ij}$  Used in This Work**

	$\varepsilon_{ij}$ (kg mol <sup>-1</sup> )	ref
$\varepsilon_{\text{PuO}_2^+, \text{ClO}_4^-}$	(0.24 ± 0.05)	1
$\varepsilon_{\text{NpO}_2^+, \text{ClO}_4^-}$	(0.25 ± 0.05)	1
$\varepsilon_{\text{PuO}_2^+, \text{Cl}^-}$	(0.09 ± 0.05)	1
$\varepsilon_{\text{NpO}_2^+, \text{Cl}^-}$	(0.09 ± 0.05)	1 <sup>a</sup>
$\varepsilon_{\text{PuO}_2^+, \text{SO}_4^{2-}}$	-(0.08 ± 0.20)	1 <sup>b</sup>
$\varepsilon_{\text{NpO}_2^+, \text{SO}_4^{2-}}$	-(0.08 ± 0.20)	1 <sup>b</sup>
$\varepsilon_{\text{PuO}_2\text{SO}_4^-, \text{Na}^+}$	(0.14 ± 0.12)	this work
	(0.02 ± 0.10)	this work <sup>c</sup>
$\varepsilon_{\text{NpO}_2\text{SO}_4^-, \text{Na}^+}$	(0.14 ± 0.17)	this work
	(0.02 ± 0.10)	this work <sup>c</sup>
	-(0.33 ± 0.19)	1
$\varepsilon_{\text{SO}_4^{2-}, \text{Na}^+}$	-(0.20 ± 0.10)	this work <sup>d</sup>
$\varepsilon_{\text{Cl}^-, \text{Na}^+}$	(0.03 ± 0.01)	1

<sup>a</sup> Assumption of  $\varepsilon_{\text{NpO}_2^+, \text{Cl}^-} = \varepsilon_{\text{PuO}_2^+, \text{Cl}^-}$ . <sup>b</sup> Estimated with the method of Vitorge et al.<sup>32</sup> <sup>c</sup> Estimated with the method of Ciavatta.<sup>31</sup> <sup>d</sup> Average value of  $\varepsilon_{\text{SO}_4^{2-}, \text{Na}^+}$  in the  $I_m = 0.357$ – $1.617$  mol kg<sup>-1</sup> range calculated as  $\varepsilon_{\text{SO}_4^{2-}, \text{Na}^+} = \varepsilon_1 + \varepsilon_2 \log I_m$  ( $\varepsilon_1 = -(0.184 \pm 0.002)$  and  $\varepsilon_2 = 0.139 \pm 0.006$ ).

where X and N are, respectively, the anion and the cation of the medium salt. Deviation of  $\pm 0.04$  kg mol<sup>-1</sup> (from 27 complexes) has been observed for  $\varepsilon_{ij}$ .<sup>31</sup> However, the uncertainties have been increased to  $\pm 0.10$  kg mol<sup>-1</sup> in the treatment of our data. Vitorge et al. have also empirically established dependence between the interaction coefficients of species of the same charge:<sup>32</sup>

$$\varepsilon_{\text{NpO}_2^+, \text{X}^-} = \varepsilon_{\text{Na}^+, \text{X}^-} + 0.12 \quad (12)$$

However, it leads only to a rough estimation and a large uncertainty was associated with it ( $\pm 0.20$  kg mol<sup>-1</sup>).

The standard binding constant,  $\log_{10} \beta_{\text{ML}_i}^0$ , was determined by an iterative procedure that minimizes the square sum of the difference between the overall mobility  $\mu_{\text{ov}}$  obtained from experimental data and that calculated from eq 5. Hence,  $\beta_{\text{ML}_i}$  was deduced from  $\beta_{\text{ML}_i}^0$  and  $\Delta(\varepsilon_{ij} m_j)$  (eqs 9 and 10), and new  $\beta_{\text{ML}_i}^0$  values were calculated. The uncertainties associated were given by a sensitive analysis, by varying simultaneously  $\mu_{\text{AnO}_2^+}$ ,  $\mu_{\text{ov}}$ ,  $[\text{Cl}^-]$ , and  $\Delta(\varepsilon_{ij} m_j)$  within their uncertainties.

When the impact of the substitution of the perchlorate ions by L is negligible on  $\Delta(\varepsilon_{ij} m_j)$ , this term is simplified as  $\Delta\varepsilon_{ij} I_m$  and  $\Delta\varepsilon_{ij}$  written as

$$\Delta\varepsilon_{ij} = -\varepsilon_{\text{Cl}^-, \text{Na}^+} - \varepsilon_{\text{AnO}_2^+, \text{ClO}_4^-} \quad (13)$$

for the equilibrium in eq 1 and

$$\Delta\varepsilon_{ij} = \varepsilon_{\text{AnO}_2\text{SO}_4^-, \text{Na}^+} - \varepsilon_{\text{SO}_4^{2-}, \text{Na}^+} \varepsilon_{\text{AnO}_2^+, \text{ClO}_4^-} \quad (14)$$

for the equilibrium in eq 2.

In this way,  $\beta_{\text{ML}_i}$  and  $\Delta\varepsilon_{ij}$  are constant in each experiment. A linear fitting was applied (eq 8) to extrapolate the standard constant  $\beta_{\text{ML}_i}^0$  and to determine  $\Delta\varepsilon_{ij}$ . The associated uncertainties were given at a 95% confidence level.

In the case of sulfate ligand, when considering the substitution of the perchlorate ions by the sulfate ions,  $\Delta(\varepsilon_{ij} m_j)$  (eq 10) was calculated from the  $\varepsilon_{\text{AnO}_2\text{SO}_4^-, \text{Na}^+} = 0.02 \pm 0.10$  kg mol<sup>-1</sup> (eq 11) and  $\varepsilon_{\text{AnO}_2^+, \text{SO}_4^{2-}} = -(0.08 \pm 0.20)$  kg mol<sup>-1</sup> (eq 12) rough

**Table 3.**  $\Delta(\varepsilon_{ij}m_j)$  and  $\log_{10} \beta_{\text{AnO}_2\text{Cl}}$  Calculated for Np and Pu<sup>a</sup>

[Cl <sup>-</sup> ] (M)	$\Delta(\varepsilon_{ij}m_j)$ (Np)	$\log_{10} \beta_{\text{NpO}_2\text{Cl}}$	$\Delta(\varepsilon_{ij}m_j)$ (Pu)	$\log_{10} \beta_{\text{PuO}_2\text{Cl}}$
0.00	$-(0.29 \pm 0.06)$	$-(0.22 \pm 0.07)$	$-(0.28 \pm 0.06)$	$-(0.23 \pm 0.07)$
0.01	$-(0.29 \pm 0.06)$	$-(0.22 \pm 0.07)$	$-(0.28 \pm 0.06)$	$-(0.23 \pm 0.07)$
0.05	$-(0.29 \pm 0.06)$	$-(0.23 \pm 0.07)$	$-(0.28 \pm 0.06)$	$-(0.24 \pm 0.07)$
0.15	$-(0.27 \pm 0.06)$	$-(0.25 \pm 0.07)$	$-(0.26 \pm 0.06)$	$-(0.26 \pm 0.07)$
0.30	$-(0.24 \pm 0.06)$	$-(0.27 \pm 0.07)$	$-(0.24 \pm 0.06)$	$-(0.28 \pm 0.07)$
0.50	$-(0.21 \pm 0.06)$	$-(0.31 \pm 0.07)$	$-(0.20 \pm 0.06)$	$-(0.32 \pm 0.07)$
0.85	$-(0.15 \pm 0.06)$	$-(0.37 \pm 0.07)$	$-(0.15 \pm 0.06)$	$-(0.38 \pm 0.07)$
1.00	$-(0.12 \pm 0.06)$	$-(0.40 \pm 0.07)$	$-(0.12 \pm 0.06)$	$-(0.40 \pm 0.07)$

<sup>a</sup> Equations 8 and 9,  $I = 1$  M, using SIT parameters in Table 2.

estimations (Table 2). The strong uncertainties associated with these estimated parameters do not allow for improvement of the accuracy of the fitting process. Therefore, it was preferred to neglect the medium variation for the data treatment.

In the case of chloride ligand, the SIT parameters are well established (Table 2),<sup>1</sup> and the  $\Delta(\varepsilon_{ij}m_j)$  values change from about  $-0.3$  in 1 M NaCl to  $-0.12$  in 1 M NaClO<sub>4</sub> (Table 3) evidencing the need to take the medium variation into account. A deviation of  $\pm 0.06$  is observed on  $\Delta(\varepsilon_{ij}m_j)$  when varying the SIT parameters (Table 2) (eq 9) within their uncertainties.

## EXPERIMENTAL SECTION

**Apparatus and Interface.** A commercial Beckman Coulter P/ACE MDQ capillary electrophoresis system (Fullerton) equipped with a UV detection mode was used for all the separations. It was provided with a tailor-made capillary cartridge support designed for the adaptation of an external detector. Conventional fused-silica 50  $\mu\text{m}$  internal diameter capillaries (Beckman Coulter, Fullerton) of 60 cm lengths were used for the separations. An optical window is located at 10.3 cm from the capillary inlet. The capillary was maintained at a constant temperature, close to 25 °C, thanks to a liquid coolant wrapping the capillary. The capillary outlet is located at 1 mm behind the nose of the nebulizer in order to ensure the electrical continuity of the circuit. Only a small portion of the capillary, outside the CE apparatus, is not temperature-controlled (Figure 1). New fused silica capillaries were preconditioned prior to use by rinsing with 1 M HCl (Prolabo, Titrimorm), 1 M NaOH (Prolabo, Titrimorm), and deionized water. The capillary was daily rinsed with 1 M NaOH and water prior to the experiments.

An Axiom (VG Elemental, Winsford, Cheshire, U.K.) inductively coupled plasma sector field mass spectrometer (ICP-SF-MS) was coupled with the capillary electrophoresis. The intrinsic detection limit is about  $10^{-16}$  M.<sup>20</sup> In the hyphenated mode, the detection limit is close to  $10^{-12}$  M. A commercial parallel path micronebulizer (Mira Mist CE, Burgener, Mississauga, Canada), which operates with a makeup liquid (2% HNO<sub>3</sub>, 10% EtOH, 1 ppb Bi as an internal standard), interfaces both apparatus. Ethanol improves the signal stability by decreasing the superficial tension of water droplets. The makeup liquid is introduced thanks to a syringe pump (11 Pico Plus, Harvard Apparatus, Holliston, Massachusetts) at a nominal flow rate of 9  $\mu\text{L min}^{-1}$ . The nebulizer is connected to a borosilicate spray chamber (Mini glass chamber, Burgener, Mississauga, Canada) (Figure 1). The ICPMS operates in the low-resolution mode ( $R = 362$ ). Bi is used to check the variation of sensitivity during the experiments.

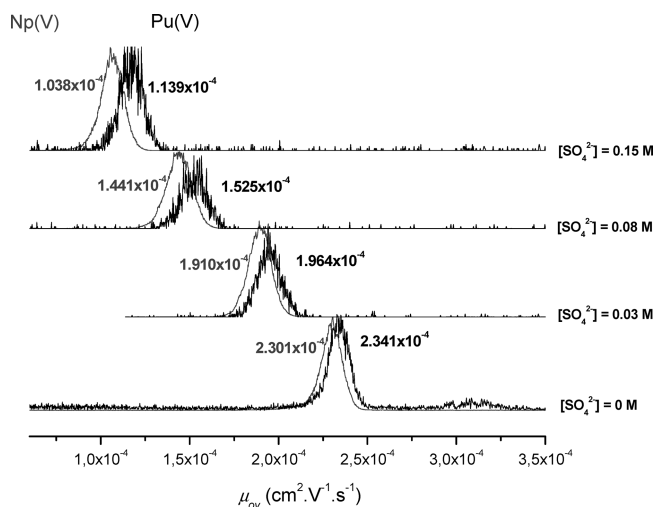


**Figure 2.** Electrophoretic mobilities of Pu(V) and Np(V) measured in (Na<sub>2</sub>SO<sub>4</sub>/NaClO<sub>4</sub>) media.  $I = 0.7$  M. The ( $2 \times 10^{-9}$  M) Pu signal is normalized to the ( $2 \times 10^{-7}$  M) Np signal intensity.

**Electrolyte and Sample Preparation.** Stock solutions of <sup>237</sup>Np in 0.1 M perchloric acid was used. Neptunium was purified on an anionic resin and then precipitated at the +5 oxidation state as NpO<sub>2</sub>OH,  $x\text{H}_2\text{O}$  ( $x \sim 2.5$ ). A  $10^{-5}$  M Np(V) stock solution was prepared in HClO<sub>4</sub> by dissolving an appropriate mass of NpO<sub>2</sub>OH,  $x\text{H}_2\text{O}$ . The oxidation state of Np into the stock solutions has been checked as +5 by spectrophotometry.

A <sup>239</sup>Pu(V) stock solution was prepared according to the following procedure: 0.5 mL of  $3 \times 10^{-7}$  M in 4 M HNO<sub>3</sub> was evaporated to dryness in a Teflon beaker. Then 2 mL of 70% HClO<sub>4</sub> was added, and the solution was white fumed at 400 °C. Caution: Note that evaporating a concentrated HClO<sub>4</sub> solution may cause an explosion, especially in the presence of organic materials (even at a trace level). Do not perform this procedure with a larger volume of concentrated HClO<sub>4</sub> solution and make sure that no organic materials are present.<sup>33</sup> This step was repeated twice in order to fully oxidize Pu(IV). This procedure allows one to rapidly obtain Pu(VI).<sup>34</sup> Finally the residue was dissolved in 1 mL of 0.7 M NaClO<sub>4</sub> solution prepared from a weighed amount of NaClO<sub>4</sub> (Merck, sodium perchlorate monohydrate). Pu(VI) is spontaneously reduced to the pentavalent state and is stable over several days.<sup>35</sup> The final concentration of Pu(V) varied from  $10^{-8}$  to  $10^{-7}$  M depending on the quality of the preparation. Because of the high sensitivity of ICPMS, it was not necessary to optimize the procedure. The absence of other oxidation states was assessed by the presence of only one typical peak on the electropherograms (Figures 2 and 3).<sup>5</sup>

Background electrolytes (BGE) were prepared from weighed amounts of Na<sub>2</sub>SO<sub>4</sub> or NaCl (Prolabo, Normapur,  $\geq 99.5\%$ ) and NaClO<sub>4</sub> dissolved in Millipore deionized water (Alpha-Q, 18.2 M $\Omega$  cm). Various concentrations of sulfate (from 0 to 0.15 M) and chloride (from 0 to 1 M) were obtained. The ionic strength

(33) Wilson, R. E.; Hu, Y.-J.; Nitsche, H. *Radiochem. Acta* **2005**, *93*, 203–205.

(34) Transurane D. 1. In *Gmelin Handbuch der Anorganischen Chemie*; Gmelin, L., Ed. Springer Verlag: Berlin, Germany, 1975; pp 27–105.

(35) Neck, V.; Altmaier, M.; Seibert, A.; Yun, J. I.; Marquardt, C. M.; Fanghanel, T. *Radiochim. Acta* **2007**, *95*, 193–207.

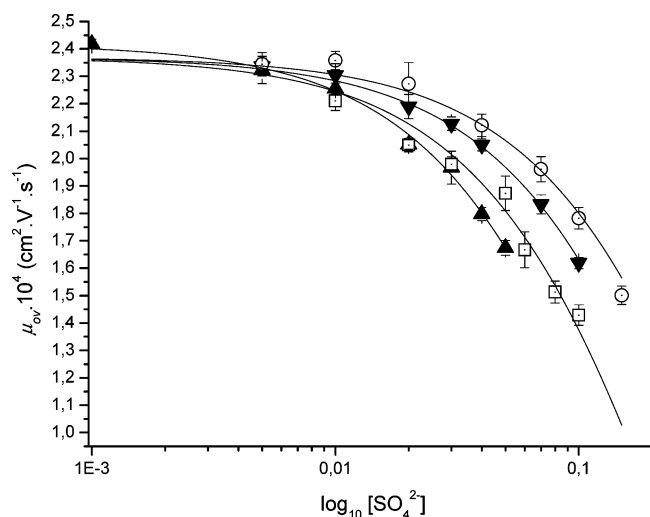


**Figure 3.** Influence of the sulfate concentration on the Pu electrophoretic mobilities in ( $\text{Na}_2\text{SO}_4/\text{NaClO}_4$ ) media at four different ionic strengths:  $I_m = 0.357$  ( $\blacktriangle$ ),  $0.725$  ( $\square$ ),  $1.051$  ( $\blacktriangledown$ ), and  $1.617$  ( $\circ$ ) mol  $\text{kg}^{-1}$ . The curves are plotted using eq 5 and the associated  $\beta_{\text{PuO}_2\text{SO}_4^-}$  and  $\mu_{\text{PuO}_2\text{SO}_4^-}$  fitted parameters (Tables 4 and 5).

(I) was adjusted with  $\text{NaClO}_4$ . The pH was close to 6 in all the experiments. Samples were prepared by mixing  $20 \mu\text{L}$  of the Pu(V) solution,  $80 \mu\text{L}$  of the BGE,  $0.2 \mu\text{L}$  of DMF (BDH, AnalaR,  $\geq 99.5\%$ ), and  $0.2 \mu\text{L}$  of the Np stock solution.

**Separation by Capillary Electrophoresis.** Before each run, the capillary was washed with BGE during 5 min at 20 psi. The separations were achieved within 15 min. The sample injections were hydrodynamically carried out at 1 psi during 4 s. The separations were performed at  $+10 \text{ kV}$  ( $I = 0.35 \text{ M}$ ),  $+7 \text{ kV}$  ( $I = 0.7 \text{ M}$ ), and  $+5 \text{ kV}$  ( $I = 1 \text{ M}$  and  $I = 1.5 \text{ M}$ ) at a constant pressure of 0.8 psi (to avoid clogging). The voltage value was chosen with respect to Ohm's law. The buffer vial was changed every run to avoid effects of electrolysis.

The determination of the temperature excess due to Joule heating is important in CE. Under our experimental conditions and in the worst case, the temperature excess has been determined as  $\Delta T = 0.90 \text{ }^\circ\text{C}$  between the center of the capillary and the liquid coolant.<sup>36</sup> The gradient of the temperature inside the capillary did not exceed  $0.3$ .<sup>36</sup> The temperature is therefore considered as homogeneous across the capillary. In conclusion, the temperature is  $25 \text{ }^\circ\text{C} \pm 1 \text{ }^\circ\text{C}$  in all experiments.

## RESULTS AND DISCUSSION

**Sulfate Complexation. Results.** The overall measured mobilities ( $\mu_{\text{ov}}$ ) of Np and Pu regularly decrease with increasing the ligand concentrations, by a factor 2 at the highest ( $0.15 \text{ mol L}^{-1}$ ) sulfate concentration (Figure 2 and Table 4), evidencing the decrease of the overall charge of the main migrating species as expected for the formation of complexes with the sulfate dianion. However,  $\mu_{\text{ov}}$  is always positive indicating that the  $\text{AnO}_2^+$  cations were predominating over the anionic sulfate complexes during all the experiments: this illustrates the weakness of the complexes and suggests that only 1–1 complexes were formed in non-negligible concentrations.

A single mobility peak is observed in each experiment: the kinetic of ligand exchange is too fast to separate the complex and the free species even for a higher voltage and longer capillary. This is consistent with labile complexes. The Np and Pu mobility results are very similar: the expected analogy between Pu(V) and Np(V) is observed, and since Np is very stable in the +5 oxidation state, this analogy also confirms that Pu was stable in the +5 oxidation state during the measurements.

However, the mobility of the aquo ion is slightly higher for  $\text{PuO}_2^+$  than for  $\text{NpO}_2^+$  (Table 4). This can be attributed to slightly higher density of charge for  $\text{PuO}_2^+$ , since the size of the ions are expected to slightly decrease with the atomic number across the actinide series. Conversely, the Np mobilities also decrease a little more than the Pu ones when increasing the sulfate concentration (Figure 2), evidencing slightly stronger complexation for Np than for Pu.

The influence of the ionic strength is quite small on the mobilities of  $\text{AnO}_2^+$ ,  $\mu_{\text{AnO}_2^+} \approx (2.37 \pm 0.08) \times 10^{-4} \text{ cm}^2 \text{ V}^{-1} \text{ s}^{-1}$  in the  $I_m = 0.357$  to  $1.617 \text{ mol kg}^{-1}$  range investigated here (Table 4). This is consistent with the usual behavior of such mobilities as a function of  $I_m$ :<sup>37–39</sup> a fast decrease of the mobility with  $I_m$  is often observed at low  $I_m$  ( $I_m < 0.2 \text{ mol kg}^{-1}$ ) prior to reaching a plateau. This value also allows one to avoid potential attribution of the peak to species at the 3+ or 4+ oxidation states. Indeed, at pH 6, An(III) and An(IV) are fully hydrolyzed or precipitated and formed only neutral species of null mobility. The  $\mu_{\text{ov}} \approx (2.37 \pm 0.08) \times 10^{-4} \text{ cm}^2 \text{ V}^{-1} \text{ s}^{-1}$  value could also potentially be attributed to An(VI), but An(VI) interacts much stronger with sulfate ligand than An(V) ( $\log_{10} \beta_{\text{An(VI)SO}_4^-}^{\text{VI}} = 3.38 \pm 0.20$  and  $3.28 \pm 0.06$  for Pu and Np, respectively)<sup>1</sup> and widely negative  $\mu_{\text{ov}}$  values should be reached in the present condition. In addition, the oxidation of Np(V) into Np(VI) requires acidic conditions and a strong oxidizing agent. Finally, the  $\mu_{\text{NpO}_2^+}$  values, found in this study, are consistent with the standard value,<sup>40</sup>  $\mu_{\text{NpO}_2^+}^0 = (2.94 \pm 0.08) \times 10^{-4} \text{ cm}^2 \text{ V}^{-1} \text{ s}^{-1}$ , and with the  $\mu_{\text{NpO}_2^+} = (2.1 \pm 0.2) \times 10^{-4} \text{ cm}^2 \text{ V}^{-1} \text{ s}^{-1}$  value at  $I = 2.5 \times 10^{-2} \text{ mol L}^{-1}$ , previously determined.<sup>29</sup>

The influence of the sulfate concentration on the measured mobilities was modeled assuming the formations of the  $\text{AnO}_2\text{SO}_4^-$  anionic 1–1 complexes (eq 5). This modeling reproduces the experimental observations (Figure 3). The  $\beta_{\text{AnO}_2\text{SO}_4^-}$  binding constants are determined by curve fitting at each ionic strength for each actinide (Figure 3).

The fitted  $\log_{10} \beta_{\text{AnO}_2\text{SO}_4^-}$  values decrease from  $(0.66 \pm 0.11)$  to  $(0.31 \pm 0.11)$  for Np and from  $(0.63 \pm 0.11)$  to  $(0.26 \pm 0.11)$  for Pu when  $I_m$  increases from  $0.357$  to  $1.617 \text{ mol kg}^{-1}$  (Table 5). This ionic strength influence is small and similar for both actinides:  $\Delta \log_{10} \beta_{\text{AnO}_2\text{SO}_4^-} = 0.35$  and  $0.37$  for Np and Pu, respectively. The  $\log_{10} \beta_{\text{AnO}_2\text{SO}_4^-}$  values seem to be the same for Np and Pu within uncertainties at each ionic strength as can be seen by  $\log_{10} K_{(\text{Np/Pu})\text{O}_2\text{SO}_4^-} = 0.03$  (for  $I_m = 0.357 \text{ mol kg}^{-1}$ ),  $0.05$  (for  $I_m = 0.725 \text{ mol kg}^{-1}$ ),  $0.03$  (for  $I_m = 1.051 \text{ mol kg}^{-1}$ ).

(37) Janz, G. J.; Olivier, B. G.; Lakshminarayanan, G. R.; Mayer, G. E. *J. Phys. Chem.* **1970**, *74*, 1285.

(38) Tanaka, K.; Hashitani, T. *Trans. Faraday Soc.* **1971**, *67*, 2314.

(39) Iadicco, N.; Paduano, L.; Vitagliano, V. *J. Chem. Eng. Data* **1996**, *41*, 529–533.

(40) Delorme, A. Le Couplage Électrophorèse Capillaire Spectromètre de Masse à Source Plasma en Tant qu'Instrument de Spéciation des Actinides à l'État de Traces. Thesis, Paris 11, Orsay, 2004.

(36) Grossman, P. D.; Colburn, J. C., Eds. *Capillary Electrophoresis Theory and Practice*; Academic Press: San Diego, CA, 1992.

**Table 4. Overall Electrophoretic Mobilities of Np and Pu in Sulfate Media<sup>a</sup>**

[SO <sub>4</sub> <sup>2-</sup> ] (M)	$\mu_{ov} \times 10^4 (\text{cm}^2 \text{V}^{-1} \text{s}^{-1})$							
	$I_m = 0.357 \text{ mol kg}^{-1}$		$I_m = 0.725 \text{ mol kg}^{-1}$		$I_m = 1.051 \text{ mol kg}^{-1}$		$I_m = 1.617 \text{ mol kg}^{-1}$	
	Np	Pu	Np	Pu	Np	Pu	Np	Pu
0.000	2.381 ± 0.016	2.424 ± 0.015	2.322 ± 0.030	2.360 ± 0.027	2.372 ± 0.053	2.405 ± 0.058	2.368 ± 0.038	2.400 ± 0.047
0.001	2.373 ± 0.016	2.418 ± 0.017						
0.005	2.276 ± 0.049	2.323 ± 0.050			2.284 ± 0.033	2.336 ± 0.031	2.301 ± 0.044	2.344 ± 0.043
0.010	2.201 ± 0.014	2.255 ± 0.020	2.165 ± 0.028	2.210 ± 0.035	2.254 ± 0.029	2.304 ± 0.042	2.312 ± 0.037	2.358 ± 0.033
0.020	1.991 ± 0.031	2.051 ± 0.017	2.000 ± 0.025	2.049 ± 0.025	2.124 ± 0.029	2.190 ± 0.044	2.226 ± 0.076	2.272 ± 0.079
0.030	1.943 ± 0.026	1.967 ± 0.060	1.929 ± 0.042	1.979 ± 0.027	2.075 ± 0.015	2.127 ± 0.025		
0.040	1.716 ± 0.019	1.797 ± 0.024			1.983 ± 0.015	2.050 ± 0.022	2.068 ± 0.027	2.121 ± 0.041
0.050	1.591 ± 0.027	1.674 ± 0.027	1.800 ± 0.064	1.873 ± 0.063				
0.060			1.588 ± 0.053	1.667 ± 0.066				
0.070					1.757 ± 0.038	1.833 ± 0.035	1.895 ± 0.049	1.961 ± 0.046
0.080			1.436 ± 0.038	1.513 ± 0.040				
0.100			1.356 ± 0.023	1.429 ± 0.037	1.582 ± 0.020	1.619 ± 0.020	1.696 ± 0.036	1.782 ± 0.039
0.150							1.414 ± 0.035	1.501 ± 0.034

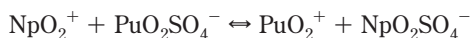
<sup>a</sup>  $T = 25 \pm 1$  °C. Uncertainties at the 95% confidence level. Mobilities are expressed with three digits after the decimal point, regardless of the significance of the last digit.

**Table 5. Stability Constants  $\log_{10} \beta_{\text{AnO}_2\text{SO}_4^-}$  Related to the Equilibrium  $\text{AnO}_2^+ + \text{SO}_4^- \leftrightarrow \text{AnO}_2\text{SO}_4^-$ <sup>a</sup>**

method	$I$	$T$ (°C)	$\log_{10} \beta_{\text{NpO}_2\text{SO}_4^-}$	$\log_{10} \beta_{\text{PuO}_2\text{SO}_4^-}$	ref
dis	2 M NaClO <sub>4</sub>	25	(0.44 ± 0.09)		10
coprecipitation	1.5 M NH <sub>4</sub> Cl	20 ± 2	(1.04 ± 0.4)		6
dis	8.5 M NaClO <sub>4</sub>	25	0.45		11
dis	0.520 m NaClO <sub>4</sub>	25	-(0.10 ± 0.08)		8
dis	1.050 m NaClO <sub>4</sub>	25	(0.06 ± 0.04)		8
dis	2.2 m NaClO <sub>4</sub>	25	(0.19 ± 0.08)		8
dis	1 M NaClO <sub>4</sub>	25	(0.76 ± 0.04)		15
recalc	2.2 m NaClO <sub>4</sub>	25	(0.45 ± 0.01)		1 <sup>b</sup>
CE-ICPMS	0.357 m NaClO <sub>4</sub>	25 ± 1	(0.66 ± 0.11)	(0.63 ± 0.11)	this work
CE-ICPMS	0.725 m NaClO <sub>4</sub>	25 ± 1	(0.54 ± 0.12)	(0.49 ± 0.12)	this work
CE-ICPMS	1.051 m NaClO <sub>4</sub>	25 ± 1	(0.40 ± 0.11)	(0.37 ± 0.11)	this work
CE-ICPMS	1.617 m NaClO <sub>4</sub>	25 ± 1	(0.31 ± 0.11)	(0.26 ± 0.11)	this work
extrapolation	0 m	25	(0.44 ± 0.27)		1 <sup>c</sup>
extrapolation	0 m	25 ± 1	(1.34 ± 0.12)	(1.30 ± 0.06)	this work <sup>d</sup>
extrapolation	0 m	25 ± 1	(1.32 ± 0.10)	(1.26 ± 0.12)	this work <sup>e</sup>

<sup>a</sup> dis, distribution between two phases; m (mol kg<sup>-1</sup>), M (mol L<sup>-1</sup>). <sup>b</sup> Calculated by the TDBP from the work of Rao et al.<sup>10</sup> <sup>c</sup> Extrapolated from the data of Halperin et al.<sup>8</sup> and Rao et al.<sup>10</sup> <sup>d</sup> Extrapolated using the simplified SIT formula (eqs 8 and 14) (medium considered as constant). <sup>e</sup> Extrapolated using the full SIT formula (eqs 8 and 10).

kg<sup>-1</sup>), and 0.05 (for  $I_m = 1.617 \text{ mol kg}^{-1}$ ), where  $K_{(\text{Np/Pu})\text{O}_2\text{SO}_4^-} = \beta_{\text{NpO}_2\text{SO}_4^-} / \beta_{\text{PuO}_2\text{SO}_4^-}$  is the constant related to the exchange equilibrium:



However, since Np and Pu were measured in the same samples, the accuracy of  $K_{(\text{Np/Pu})\text{O}_2\text{SO}_4^-}$  is better than those of  $\beta_{\text{NpO}_2\text{SO}_4^-}$  and  $\beta_{\text{PuO}_2\text{SO}_4^-}$ : the 0.03 to 0.05  $\log_{10} K_{(\text{Np/Pu})\text{O}_2\text{SO}_4^-}$  values are meaningful; they directly correspond to the shift between the Np and Pu peaks (Figure 2), evidencing the higher stability of the Np complex and might be attributed to some covalency.

The overall mobilities are clearly dependent on the ionic strength (Figure 3): for a given sulfate concentration,  $\mu_{ov}$  decreases with the ionic strength, indicating a destabilization of the complex, as reflected in the  $\log_{10} \beta_{\text{AnO}_2\text{SO}_4^-}$  values, which decrease by about 0.36  $\log_{10}$  units from  $I_m = 0.357 \text{ mol kg}^{-1}$  to  $I_m = 1.617 \text{ mol kg}^{-1}$ . Since the  $\text{AnO}_2^+$  reactant and the  $\text{AnO}_2\text{SO}_4^-$  product are both monoions, the effects of their activity coefficients cancel out to a certain extent: the main ionic strength effect is due to the decrease of the activity of the  $\text{SO}_4^{2-}$  ligand with the ionic strength. Plotting  $\log_{10} \beta_{\text{AnO}_2\text{SO}_4^-} + 4D$  (eq

8) versus  $I_m$ , a linear curve is obtained, in which the intercept is  $\log_{10} \beta_{\text{AnO}_2\text{SO}_4^-}^0$  and the slope is  $\Delta\varepsilon_{ij}$  (Figures 4 and 5):  $\log_{10} \beta_{\text{NpO}_2\text{SO}_4^-}^0 = 1.34 \pm 0.12$ ,  $\Delta\varepsilon_{ij} = 0.10 \pm 0.12 \text{ kg mol}^{-1}$  (Pu) and  $\Delta\varepsilon_{ij} = 0.09 \pm 0.12 \text{ kg mol}^{-1}$  (Np). These standard constants are similar to those determined when considering the variations of the SIT term (addition of the term  $\varepsilon_{\text{AnO}_2^+, \text{SO}_4^{2-}}$  (eq 10)),  $\log_{10} \beta_{\text{PuO}_2\text{SO}_4^-}^0 = 1.26 \pm 0.12$  and  $\log_{10} \beta_{\text{NpO}_2\text{SO}_4^-}^0 = 1.32 \pm 0.10$ . The  $\log_{10} \beta_{\text{AnO}_2\text{SO}_4^-}^0$  varies from about 1.2 to 1.4 when extrapolated using the lower and the higher  $\log_{10} \beta_{\text{AnO}_2\text{SO}_4^-}$  values, respectively (Table 5), while  $\Delta\varepsilon_{ij}$  remains similar ( $\approx -(0.10 \pm 0.12) \text{ kg mol}^{-1}$ ).

From the fitted values of  $\Delta\varepsilon_{ij}$ ,  $\varepsilon_{\text{NpO}_2\text{SO}_4^-, \text{Na}^+} = 0.14 \pm 0.17 \text{ kg mol}^{-1}$  and  $\varepsilon_{\text{PuO}_2\text{SO}_4^-, \text{Na}^+} = 0.14 \pm 0.17 \text{ kg mol}^{-1}$  are calculated (eq 14). These are strongly dependent on the other SIT parameters as reflected in the propagated error (Table 2). The  $\varepsilon_{\text{AnO}_2\text{SO}_4^-, \text{Na}^+}$  values found here are in fair agreement with those often tabulated for an interaction between a monoanion and  $\text{Na}^+$  (between 0.05 and  $-0.05 \text{ kg mol}^{-1}$ ),<sup>1</sup>  $\varepsilon_{\text{OH}^-, \text{Na}^+} = 0.04 \pm 0.01 \text{ kg mol}^{-1}$ ,  $\varepsilon_{\text{Am}(\text{SO}_4)_2^-, \text{Na}^+} = -(0.05 \pm 0.05) \text{ kg mol}^{-1}$ ,  $\varepsilon_{\text{UO}_2\text{F}_3^-, \text{Na}^+} = 0.00 \pm 0.05 \text{ kg mol}^{-1}$ , and with the one calculated using the model of Ciavatta (eq 11),  $\varepsilon_{\text{AnO}_2\text{SO}_4^-, \text{Na}^+} = 0.02 \pm 0.10 \text{ kg mol}^{-1}$ .

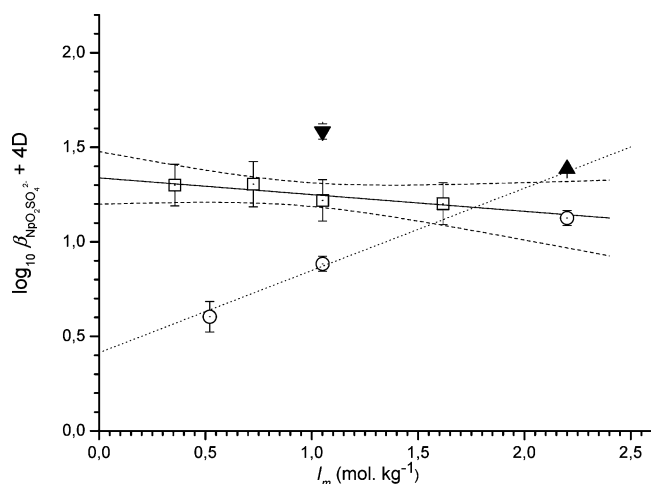


**Figure 4.** Extrapolation of the binding constants  $\log_{10} \beta_{\text{NpO}_2\text{SO}_4^-} + 4D$  to zero ionic strength using the SIT formula (eq 13) in this work ( $\square$ , solid line) and as published by the NEA review from older data of different authors ( $\blacktriangle$ ,<sup>10</sup>  $\circ$ ,<sup>8</sup> dotted line) discarding one of them ( $\blacktriangledown$ <sup>15</sup>).

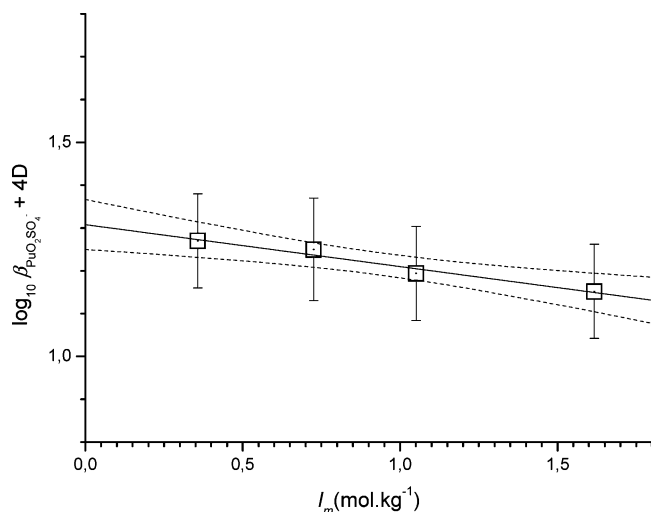


**Figure 5.** Extrapolation of the binding constants  $\log_{10} \beta_{\text{PuO}_2\text{SO}_4^-} + 4D$  to zero ionic strength using the SIT formula (eq 13).

**Discussion.** All the previous investigations make only reference to the formation of the  $\text{NpO}_2\text{SO}_4^-$  1–1 complex. Our  $\log_{10} \beta_{\text{NpO}_2\text{SO}_4^-} = 0.40 \pm 0.11$  value (Table 5) at about 1 M ionic strength is between the two published values ( $0.06 \pm 0.04$ )<sup>8</sup> and ( $0.76 \pm 0.04$ )<sup>15</sup> determined by liquid–liquid extraction in the same medium. Inoue et al. have criticized them when reviewing previous works.<sup>15</sup> The authors expressed doubt on the efficiency of the DNNS extractant.<sup>8,10,11</sup> Indeed, the authors estimate that the percentage of the Np(V) extracted is not sufficient (11–18%) to obtain a reliable binding constant. Moreover, Inoue et al. suspected the presence of  $\text{H}_2\text{O}_2$  in the experiment performed by Halperin et al., which can lead to the decrease of the apparent binding constant. Inoue et al. have used 2-thenoyltrifluoroacetone (TTA) and 1,10-phenanthroline, which allows one to obtain a better extraction of Np(V).<sup>15</sup> The authors indicate that TTA has an effect on the complexation and have corrected the distribution ratio. However, they used a buffer mixture of MES and THAM, which can also lead to a bias since MES and

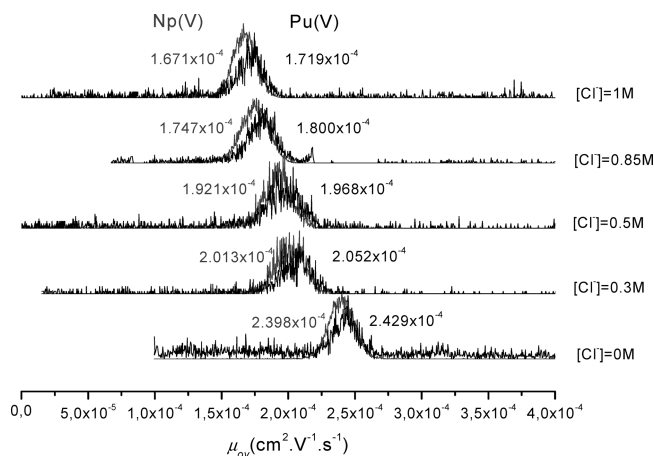


**Figure 6.** Electrophoretic mobilities of Pu and Np in (NaCl/NaClO<sub>4</sub>) media  $I = 1$  M. The ( $2 \times 10^{-9}$  M) Pu signal is normalized to the ( $2 \times 10^{-9}$  M) Np signal intensity.

**Table 6. Overall Electrophoretic Mobilities of Np and Pu in Chloride Media<sup>a</sup>**

[Cl <sup>-</sup> ] (M)	$\mu_{ov} \times 10^4$ (cm <sup>2</sup> V <sup>-1</sup> s <sup>-1</sup> )	
	Np	Pu
0.00	2.372 ± 0.053	2.405 ± 0.058
0.01	2.332 ± 0.045	2.374 ± 0.042
0.05	2.312 ± 0.035	2.339 ± 0.042
0.15	2.239 ± 0.050	2.279 ± 0.048
0.30	1.998 ± 0.040	2.034 ± 0.048
0.50	1.889 ± 0.064	1.931 ± 0.073
0.85	1.735 ± 0.063	1.771 ± 0.044
1.00	1.694 ± 0.038	1.729 ± 0.042

<sup>a</sup>  $I = 1$  M and  $T = 25 \pm 1$  °C. Uncertainties at the 95% confidence level. Mobilities are expressed with three digits after the decimal point, regardless of the significance of the last digit.

especially THAM have non-negligible metal-binding properties,<sup>41,42</sup> which may result in a higher amount of complexed Np(V).

The literature data do not exhibit a clear trend versus the ionic strength.<sup>6,8,10,11,15</sup> For Halperin et al.,  $\log_{10} \beta_{\text{NpO}_2\text{SO}_4^-} = - (0.10 \pm 0.08)$  at  $I_m = 0.52$  mol kg<sup>-1</sup>,  $\log_{10} \beta_{\text{NpO}_2\text{SO}_4^-} = 0.06 \pm 0.04$  at  $I_m = 1.05$  mol kg<sup>-1</sup>, and  $\log_{10} \beta_{\text{NpO}_2\text{SO}_4^-} = 0.19 \pm 0.08$  at  $I_m = 2.20$  mol kg<sup>-1</sup> leading to  $\log_{10} \beta_{\text{NpO}_2\text{SO}_4^-}^0 = 0.58 \pm 0.07$  and  $\Delta\epsilon_{ij} = - (0.25 \pm 0.04)$  kg mol<sup>-1</sup>.<sup>8</sup> However, it must be noted that the amount of complex formed in the experiment at  $I_m = 0.52$  mol kg<sup>-1</sup> was only about 10%, which seems too low to use this point confidently when extrapolating to zero ionic strength. For Rao et al.,  $\log_{10} \beta_{\text{NpO}_2\text{SO}_4^-} = 0.44 \pm 0.09$  at  $I = 2$  M<sup>10</sup> and Patil et al.,  $\log_{10} \beta_{\text{NpO}_2\text{SO}_4^-} = 0.45$  (no uncertainty given) at  $I = 8.5$  M,<sup>11</sup> and no variation of the binding constant with the ionic strength is noticed. The NEA proposes a  $\log_{10} \beta_{\text{NpO}_2\text{SO}_4^-}^0 = 0.44 \pm 0.27$  and  $\Delta\epsilon_{ij} = - (0.37 \pm 0.18)$  kg mol<sup>-1</sup> values<sup>1</sup> (Figure 4) based on the selected data from Halperin et al.<sup>8</sup> (including the inaccurate experiment at  $I_m = 0.52$  mol kg<sup>-1</sup>) and from Rao et al.<sup>10</sup> The difference between our  $\log_{10} \beta_{\text{NpO}_2\text{SO}_4^-}^0 = 1.34 \pm 0.12$  value and those selected by the NEA is directly assigned to the choice of data at different ionic strengths. This is illustrated by the large difference of the  $\Delta\epsilon_{ij}$  value between this work and that

(41) Good, N. E.; Winget, G. D.; Winter, W.; Connolly, T. N.; Izawa, S.; Singh, R. M. M. *Biochemistry* **1966**, *5* (2), 467–477.

(42) Machado, C. M. M.; Soares, H. M. V. M. *Talanta* **2007**, *71*, 1352–1363.

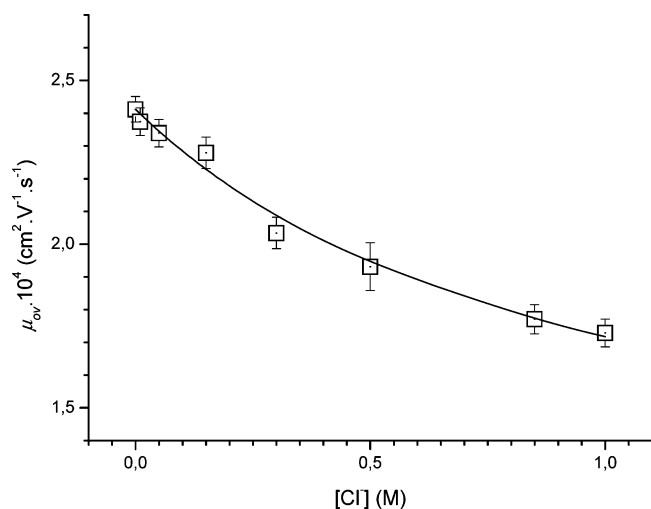


**Figure 7.** Comparison of  $\mu_{ov}$  experimentally determined ( $\square$ ) and  $\mu_{ov}$  calculated with  $\beta_{PuO_2Cl}$  (Table 3) using eq 5 (line) for Pu.

recommended by the NEA:  $\Delta\Delta\varepsilon_{ij} \approx 0.5 \text{ kg mol}^{-1}$ . The  $\varepsilon_{NpO_2SO_4^-,Na^+} = -(0.33 \pm 0.19) \text{ kg mol}^{-1}$  value calculated from the NEA extrapolation seems to be too negative in comparison with (1) the common values of  $\varepsilon_{X^-,Na^+}$  ( $-0.05 \text{ kg mol}^{-1} < \varepsilon_{X^-,Na^+} < 0.05 \text{ kg mol}^{-1}$ , where  $X^-$  is a monoanion), (2) with the  $\varepsilon_{NpO_2SO_4^-,Na^+}$  estimated using the Ciavatta model (eq 11),  $\varepsilon_{NpO_2SO_4^-,Na^+} = 0.02 \pm 0.10 \text{ kg mol}^{-1}$ , and (3) with  $\varepsilon_{NpO_2SO_4^-,Na^+} = 0.14 \pm 0.17 \text{ kg mol}^{-1}$  determined in this work (Table 2). Consequently, the NEA  $\Delta\varepsilon_{ij} = -(0.37 \pm 0.18) \text{ kg mol}^{-1}$  value might be also too negative and lead to bias in the  $\log_{10} \beta_{NpO_2SO_4^-} = 0.44 \pm 0.27$  value.<sup>1</sup>

**Chloride Complexation. Results.** The trend of the overall measured mobilities for the interaction with chloride ions is quite similar to those with sulfate: (1) a decrease of the  $\mu_{ov}$  mobilities by a factor 1.5 for both Np and Pu with increasing the ligand concentration (up to  $1 \text{ mol L}^{-1} \text{ Cl}^-$ ) (Figure 6 and Table 6), (2) overall mobilities are always positive as expected for a variation from a monocation species,  $AnO_2^+$ , to a neutral species  $AnO_2Cl$ , (3) a single peak observed indicating a weak interaction, (4) a similar mobility for Np and Pu indicating the stability of the +5 oxidation state of Pu in the sodium perchlorate/chloride medium.

However, in opposition with the sulfate medium, the Np and Pu mobilities decrease similarly when increasing the chloride concentration (Figure 6) indicating that the strength of the interaction is of the same order for Np and Pu. The influence of the chloride concentration on the measured mobilities was

modeled assuming the formation of the  $AnO_2Cl$  neutral 1–1 complexes. The  $\log_{10} \beta_{AnO_2Cl}$  values have been determined by using the iterative procedure described in the treatment of data since the medium change cannot be neglected (from 100%  $NaClO_4$  to 100%  $NaCl$ ). The  $\mu_{ov}$  experimental values fit well with the model (Figure 7), and very low  $\log_{10} \beta_{AnO_2Cl}$  ( $< 0$ ) values are obtained in each experiment (Table 7). These values vary from about  $-0.2$  to  $-0.4$  between  $1 \text{ M } NaClO_4$  and  $1 \text{ M } NaCl$  and are similar for Np and Pu (Table 6). This shift illustrates why the data treatment can not be simplified as performed for the study with sulfate. The iterative procedure converges quickly, and the standard binding constants  $\log_{10} \beta_{NpO_2Cl}^0 = -(0.12 \pm 0.13)$  and  $\log_{10} \beta_{PuO_2Cl}^0 = -(0.12 \pm 0.13)$  are obtained.

**Discussion.** The binding constants reported by the NEA are, in general, very low and quite scattered.<sup>9–12</sup> It is not surprising when considering the overall weakness of the Np and Pu binding constants with the chloride ligand:  $\log_{10} \beta_{An(V)Cl_n^{+(2-n)}}$ ,  $\log_{10} \beta_{An(V)Cl_n^{+(1-n)}}$ ,  $\log_{10} \beta_{An(IV)Cl_n^{+(4-n)}}$ ,  $\log_{10} \beta_{An(III)Cl_n^{+(3-n)}}$  are all close to 0.<sup>1</sup> The data relative to Np(V) are just quoted by the NEA without any selection. All these data were measured in high ionic strength solutions avoiding the direct comparison with our values in  $1 \text{ M } NaCl$ . Nevertheless, the obtained  $\log_{10} \beta_{NpO_2Cl} = -(0.40 \pm 0.07)$  value is of the same order of the published values,  $-(0.42 \pm 0.04)$ ,<sup>10</sup>  $-(0.29 \pm 0.05)$ ,<sup>9</sup> and  $-(0.05 \pm 0.02)$ ,<sup>12</sup> respectively, determined in  $2 \text{ M } Na(Cl, ClO_4)$ ,  $2 \text{ M } H(Cl, ClO_4)$ , and  $5 \text{ M } Na(Cl, ClO_4)$ . Doubts have been emitted by the NEA<sup>1</sup> on the correction of the activity coefficients, used by Neck et al., with the substitution of a large fraction of perchlorate ions with chloride ions.<sup>12</sup> In the same way, Gainar et al.<sup>9</sup> and Rao et al.<sup>10</sup> have not taken into account the medium change and the values obtained can be solely explained in term of activity coefficient deviation. In addition, the potentiometric investigation of Danesi et al. have not shown any interaction between  $AnO_2^+$  and the chloride ions.<sup>43</sup>

The  $\log_{10} \beta_{PuO_2Cl}^0$  and  $\log_{10} \beta_{NpO_2Cl}^0$  binding constants are found to be equal (Table 7), indicating a mainly ionic interaction between the ligand and the metal. That is confirmed by all the structural information available, which tends to show that no inner sphere interaction occurs up to  $5 \text{ M } Cl^-$ .<sup>12–14</sup>

No clear trend of the  $\log_{10} \beta_{NpO_2Cl}$  variation versus ionic strength can be extrapolated from the literature data. Furthermore, it is probably more interesting to use the data obtained in  $1 \text{ M } NaCl$ ,  $\log_{10} \beta_{AnO_2Cl} = -(0.40 \pm 0.07)$ , instead of those obtained in an infinite dilute medium,  $\log_{10} \beta_{AnO_2Cl}^0 = -(0.12 \pm 0.13)$ , since there is a significant uncertainty on the extrapola-

**Table 7. Stability Constants  $\log_{10} \beta_{AnO_2Cl}$  Related to the Equilibrium  $AnO_2^+ + Cl^- \leftrightarrow AnO_2Cl^0$**

method	<i>I</i>	<i>T</i> (°C)	$\log_{10} \beta_{NpO_2Cl}$	$\log_{10} \beta_{NpO_2Cl_2^-}$	$\log_{10} \beta_{PuO_2Cl}$	ref
dis	8.5 M $Na(Cl, ClO_4)$	25	0.48			11
dis	5 M $Na(Cl, ClO_4)$	25	$-(0.05 \pm 0.02)$	$-(0.71 \pm 0.04)$		12
sp	4 M $NaCl$	25	"no complexation"			14
emf	4 M $(Na, H)(Cl, ClO_4)$	25	"no complexation"			43
cix	2 M $H(Cl, ClO_4)$	25	$-(0.29 \pm 0.05)$			9
dis	2 M $Na(Cl, ClO_4)$	25	$-(0.42 \pm 0.04)$			10
CE–ICPMS	1 M $NaCl$	$25 \pm 1$	$-(0.40 \pm 0.07)$		$-(0.40 \pm 0.07)$	this work
CE–ICPMS	0 m	$25 \pm 1$	$-(0.12 \pm 0.13)$		$-(0.12 \pm 0.13)$	this work <sup>b</sup>

<sup>a</sup> cix, cation exchange; emf, electromotive force; dis, distribution between two phases; sp, spectrophotometry; m ( $\text{mol kg}^{-1}$ ), M ( $\text{mol L}^{-1}$ ).

<sup>b</sup> Extrapolated by using the SIT formula.

tion to zero ionic strength. Indeed, to date, there is a discussion on the SIT applicability to the weakest interactions.

## CONCLUSIONS

In this work, the high sensitivity and resolution of the CE–ICPMS technique allows one to establish, for the first time, values for the binding constant of chlorides and sulfates with Pu(V),  $\log_{10} \beta_{\text{PuO}_2\text{SO}_4^-}^0 = 1.30 \pm 0.11$  and  $\log_{10} \beta_{\text{PuO}_2\text{Cl}}^{1\text{M NaCl}} = -(0.40 \pm 0.07)$ , and to provide new values for those with Np(V),  $\log_{10} \beta_{\text{NpO}_2\text{SO}_4^-}^0 = 1.34 \pm 0.12$  and  $\log_{10} \beta_{\text{NpO}_2\text{Cl}}^{1\text{M NaCl}} = -(0.40 \pm 0.07)$ . These results seem to show that the Np(V)/Pu(V) analogy can be used confidently for electrostatic interactions (chloride ligands). Conversely, a slight shift is observed when the binding is not only electrostatic and might present some covalency (sulfate ligands). However, to confirm this trend, other ligands must be investigated (nitrate, hydroxide, . . .) as well as a full thermodynamical study by using the thermoregulation system

of the CE (15–55 °C). Moreover, the CE–ICPMS instrumentation seems to be suitable to improve speciation analysis as stressed by the legislation relative to the monitoring of chemicals in the environment.<sup>44</sup>

## ACKNOWLEDGMENT

The financial support provided by CEA/DAM/DME allowing us to couple the CE with ICPMS and to perform measurements in a clean room is greatly appreciated.

Received for review February 5, 2009. Accepted May 15, 2009.

AC900275D

(43) Danesi, P. R.; Chiariza, R.; Scibona, G.; D'Alessandro, G. *J. Inorg. Nucl. Chem.* **1974**, *36*, 2396.

(44) Rosenberg, E. *Trends Anal. Chem.* **2007**, *26*, 11.